Semisharp Phase Field Method for Quantitative Phase Change Simulations

Gustav Amberg
Department of Mechanics, KTH, S-100 44 Stockholm, Sweden
(Received 1 July 2003; revised manuscript received 15 September 2003; published 31 December 2003)

The standard phase field model for simulation of phase change requires an asymptotic analysis in a vanishing interface width, in order to connect the model parameters to the sharp interface parameters, which has hampered the quantitative usefulness of the method. In this Letter the method is simplified to the point that the relevant reduced problem can be solved analytically, allowing the sharp and phase field parameters to be identified, in principle, without restrictions on the model parameters. The scheme is tested for standard cases of two-dimensional solidification, showing excellent agreement with sharp interface kinetics.

DOI: 10.1103/PhysRevLett.91.265505 PACS numbers: 81.30.Fb, 02.60.Cb, 64.70.Dv, 81.10.Aj

The phase field method [1–3] is a widely used method to study the evolution of microstructures in phase change problems, such as dendritic growth of crystals in an undercooled melt. The governing equations are derived from the thermodynamic potentials of the system, together with the assumption of a surface energy associated with a diffuse solid/liquid interface. It is thus possible to consider different physical situations with relative ease, such as grain boundaries, mixtures, etc. It is also fairly easy to implement numerically, since interfaces are not tracked explicitly. Instead, a variable is introduced that has different constant values in the solid and liquid, and a steep transition between the two in the diffuse interface.

The problem with the method is that in its original form, the width of the diffuse interface must be prohibitively small for the results to match the proper interface kinetics [4,5], typically $W^* \ll d_0^*$, where W^* is the interface width, and $d_0^* = cT_m\gamma/L^2$ is the capillary length, which in typical cases can be in the order of nanometers (c is specific heat, T_m temperature of a flat interface at equilibrium, γ surface energy, and L latent heat). As a remedy to this, Karma and Rappel [6,7] introduced the thin interface version of the method, where the asymptotic analysis of the phase field equations is taken to second order in interface width, allowing the kinetics to be identified under less stringent conditions [6,7]. Also, in the thin interface limit the kinetic term can be eliminated from the undercooling, if that is desired. However, the seemingly modest extension of this analysis to nonhomogeneous properties, such as different diffusion coefficients in the solid and liquid, requires nontrivial modifications of the model equations [8,9]. An interesting step towards more computationally efficient methods for solidification at high undercooling was taken by Bragard *et al.* [10].

In this Letter the standard phase field method is simplified to the point that a relevant reduced problem can be solved analytically. The primary simplification is to modify the terms in the description of the energy of the system, so that the dependency of the phase field is essentially discontinuous, while maintaining a continuous potential barrier between phases. This device allows the phase change interface to be identified with the phase field contour where the sharp change in energy takes place, thus making the model in some sense "sharp." The continuous potential barrier between phases still gives a continuous variation of the phase field that can be rather wide, which is highly beneficial since it allows curvatures to be evaluated accurately. The presented method can perhaps also be viewed as an intermediate between the standard phase field formulations and proper sharp interface or level set methods, e.g., Ref. [11].

For clarity we describe the derivation of the model for the simple situation of thermal solidification of a pure material with isotropic Gibbs-Thomson kinetics at the interface, $-\theta_i = V/\mu + d_0/R$. Here V denotes the normal speed of the interface, μ the kinetic coefficient, R the local radius of curvature, and d_0 the capillary length. Here, and in the following, we have nondimensionalized temperature according to $\theta = c(T - T_m)/L$, lengths with an (arbitrary) reference length H, time with H^2/κ, where κ is the heat diffusivity.

As a starting point, the phase field model is written as

$$\tau\frac{\partial\phi}{\partial t} = W^2\nabla^2\phi - f'(\phi) - g'_\delta(\phi)h(\lambda\theta). \qquad (1)$$

Here ϕ is the phase field variable which is $+1$ in the solid and -1 in the liquid. W denotes the interface width parameter, τ is linked to the kinetic undercooling, and λ is linked to the capillary length.

The conservation of heat takes the form

$$\frac{\partial\theta}{\partial t} = \nabla^2\theta + \frac{\partial g_\delta(\phi)}{\partial t}. \qquad (2)$$

The function $f(\phi)$ should be a double well, with minima at $\phi = \pm 1$, and $g_\delta(\phi)$ accounts for the change in internal energy on phase change and should increase from 0 to 1 as ϕ goes from -1 to $+1$. A standard choice is

$f(\phi) = (1-\phi)^2(1+\phi)^2$ and $g_\delta(\phi) = 15/16(\phi^5/5 - 2\phi^3/3 + \phi) + 1/2$. We note that the two functions $f(\phi)$ and $g_\delta(\phi)$ are independent, and that there is a large degree of freedom in choosing these. Here we have also introduced a function $h(\lambda\theta)$ in the last term of Eq. (1), which in the standard model is $h(\lambda\theta) = \lambda\theta$.

We now introduce the following modifications: (i) The function $g_\delta(\phi)$ is chosen as a smoothed step function that jumps from 0 to 1 over an interval of width $\sim\delta$ at $\phi = 0$. The model we are interested in is then obtained in the limit $\delta = 0$. (ii) In order to evaluate the kinetics of the model exactly, we choose a simpler form of $f(\phi)$, i.e., $f(\phi) = (\phi - 1)^2$ for $\phi > 0$, and $f(\phi) = (\phi + 1)^2$ for $\phi < 0$. (iii) An explicit choice of the function $h(\lambda\theta)$ is made below, in order to obtain linear Gibbs-Thomson kinetics, also for large values of $\lambda\theta$. A similar function was introduced by Bragard *et al.* [10], who determined it numerically; here, however, it is found explicitly.

We view the interface as being given by the contour generated by $\phi = 0$; i.e., the interface is sharp in this sense. The crucial property is that we show that this model gives Gibbs-Thomson kinetics, with the temperature taken precisely at the point where $\phi = 0$.

We now proceed to study a reduced problem, assuming a profile of ϕ that is translating with a quasiconstant shape, in the presence of mild curvature, i.e., $R \gg W$, retaining terms of order W/R. With these approximations the phase field Eq. (1) simplifies to

$$-\tau U \frac{d\phi}{dz} = W^2 \frac{d^2\phi}{dz^2} - 2(\phi \pm 1), \tag{3}$$

where

$$\tau U = \tau V + W^2/R, \tag{4}$$

where the $+$ ($-$) sign is used in the liquid (solid). Here V is the local normal velocity of the interface, and the symbol U thus incorporates both the kinetic and the curvature terms. This equation is now valid away from the point where $\phi = 0$, and we notice that the temperature does not enter, and also that it is linear, due to the choice of f made above.

At the point where $\phi = 0$, the jump in g_δ generates a jump in the gradient of ϕ. By multiplying Eq. (1) by $d\phi/dz$ and integrating across the point where $\phi = 0$, we obtain

$$\frac{W^2}{2}\left[\left(\frac{d\phi^+}{dz}\right)^2 - \left(\frac{d\phi^-}{dz}\right)^2\right] = h(\lambda\theta_i). \tag{5}$$

Here θ_i is the value of the temperature at the interface, $\phi = 0$.

We now solve Eqs. (4), subject to boundary conditions $\phi^-(-\infty) = 1$, $\phi^-(0) = \phi^+(0) = 0$, $\phi^-(+\infty) = -1$, i.e., solidification proceeding towards increasing z, with the origin of the z axis chosen to coincide with the position of the interface. The solutions are readily obtained as

$$z < 0: \qquad \phi^- = 1 - e^{z\sigma_-}, \tag{6}$$

$$z > 0: \qquad \phi^+ = -1 + e^{z\sigma_+}, \tag{7}$$

where

$$\sigma_\mp = -\frac{\tau U}{2W^2} \pm \sqrt{\frac{2}{W^2} + \left(\frac{\tau U}{2W^2}\right)^2}. \tag{8}$$

The kinetics is now obtained by inserting the solutions (8) in the jump condition (5), the result being

$$-\frac{1}{2}\frac{\tau U}{W}\sqrt{8 + \left(\frac{\tau U}{W}\right)^2} = h(\lambda\theta_i). \tag{9}$$

Here we also see how to choose the function $h(\lambda\theta_i)$; if this is taken as the same functional form as the left-hand side, i.e., $h(\lambda\theta_i) = \frac{1}{2}\lambda\theta_i\sqrt{8 + (\lambda\theta_i)^2}$, it is seen that Eq. (9) is now satisfied if $-\lambda\theta_i = \frac{\tau U}{W}$, which gives linear kinetics, i.e., remembering the definition of U in Eq. (4) and rearranging:

$$-\theta_i = \frac{\tau V}{W\lambda} + \frac{1}{R}\frac{W}{\lambda}. \tag{10}$$

By comparing with Gibbs-Thomson kinetics, we can now identify the phase field and the sharp interface parameters as $\mu = W\lambda/\tau$ and $d_0 = W/\lambda$.

This derivation is exact in the sense that the 1D problem yields the Gibbs-Thomson kinetics for all width parameters W. The approximation involved is primarily that the transition width must be small compared to the radius of curvature, $W \ll R$.

Anisotropy was not accounted for in the derivation above, but this has been included in the same way as for the standard model, and gives the appropriate anisotropic version of the Gibbs-Thomson relation.

In order to test the performance of this method, Eqs. (1) and (2), with the addition of anisotropy, and with the special choices of $g_\delta(\phi)$ and $f(\phi)$ noted above, were implemented in 2D. This was done using finite elements on unstructured adaptive grids using our toolbox femLego [12], much in the same way as in our previous phase field simulations, e.g., Refs. [13,14]. Space does not permit a full account of the implementation details here, but the main addition is the treatment of $g'_\delta(\phi)$ in Eq. (1). The resulting jump in the square gradient of ϕ in Eq. (5), can, using the solutions (8), be enforced in finite elements by adding a line integral of $W\lambda\theta$ along the interface. This is easily implemented as a source term. We have not done the analogous finite difference solution as yet, but it should be straightforward to add a corresponding source term in a conservative manner also in a finite difference code. The discontinuity in $f'(\phi)$ is implemented as such with a simple switch. In the temperature equation, the discontinuity in $g_\delta(\phi)$ is implemented as a slightly smoothed step function, $g_\delta(\phi) = [1 + \phi\sqrt{(1+\delta^2)/(\phi^2+\delta^2)}]/2$, with a value of $\delta = 0.05$.

The implementation above is second order accurate in space except at the interface where it is first order. A proper second order accurate implementation that would allow gradient jumps inside the elements where the interface passes should give a great improvement in computational efficiency. Even so, with the present very simple implementation, the computational work is in the order of the thin interface limit method or less.

For large undercooling when the kinetic undercooling dominates, it is seen from (8) that as the interface gets thicker, i.e., λ increases, the gradient of ϕ increases ahead of the front, which may increase the need for numerical resolution. At lower undercooling when capillary undercooling dominates, the difficulty is that the temperature must be known very accurately at the interface. The gradient ahead of the front is of the order θ_∞/R, while the important temperature variations on the interface are d_0/R. This translates into a spatial resolution requirement of a mesh finer than d_0/θ_∞. Notice that this has to be satisfied by any method, unless higher order interpolation within elements crossing the interface is implemented, as discussed above.

We now show the results of a simulation of a typical case with an undercooling of 0.5, i.e., $\theta_\infty = -0.5$. The sharp interface parameters are taken as $\mu = 117.5$ and $d_0 = 0.001\,191$. We have also included anisotropy, by letting the surface energy vary by a factor $[1 + \epsilon\cos(4\beta)]$, with β being the angle between an interface normal and the preferred growth direction, in the conventional way. The value of the anisotropy parameter was $\epsilon = 0.04$. The phase field parameters λ, τ, and W are determined by the relations given below Eq. (10) and the specification of a desired interface width. Here we show results for the two cases $W = 0.02$ and 0.04, with the corresponding values $\lambda = 16.792$, $\tau = 0.002\,858$ and $\lambda = 33.58$, $\tau = 0.011\,432$. Both cases are deliberately chosen with very thick interfaces, i.e., λ considerably larger than unity.

Simulating the growth for times from 0 to 0.6, the shape evolves into a typical needle crystal, where the tip attains a nearly parabolic shape and a constant speed. Figure 1 shows a close-up view of the tip region at $t = 0.6$ for $W = 0.02$. We note that the temperature is quite smooth, and the jump in temperature gradient is very well defined. The temperature gradient changes over 1–2 elements at the interface, and the only restriction is the numerical resolution there. The region where the phase field varies is roughly the same as that where the mesh is refined, i.e., much wider than this.

As a direct check on the kinetics, the temperature θ_i at the interface $\phi = 0$ was plotted as a function of distance along the interface. The thicker black curve in Fig. 2 shows θ_i along the interface at $t = 0.6$. To obtain a simple length coordinate increasing along the interface, the values belonging to points on the interface below (above) the diagonal are plotted as functions of y (x). There is a region near the root of the crystal where the interface has negative curvature, and θ_i is consequently positive. It then decreases gradually towards the tip where the curvature and normal velocity are both maximal. As a check on the kinetics, local values of curvature, normal speed, and inclination angle were extracted from the solution, and the corresponding temperature was computed according to Eq. (10). This is shown as the thinner line in Fig. 2. In fact, the two are exactly coinciding over most of the range, showing that the correct kinetics are indeed obeyed. There is some minor noise in the thin curve arising in the poorly conditioned operation of explicitly computing curvatures, etc.

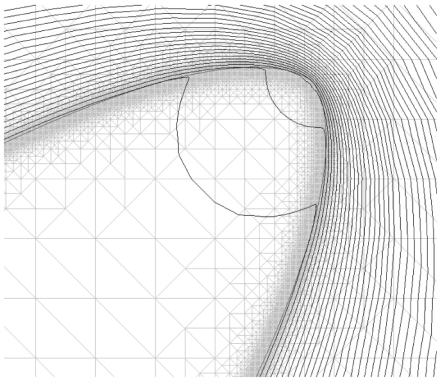

FIG. 1. Isotherms around the tip. Values on isotherms differ by 0.01.

As a check on the dependency of growth on the interface width, Fig. 3 shows contours of the phase field variable at $t = 0.6$. The contours below the diagonal are simulated with $W = 0.02$, and the contours above for $W = 0.04$. We notice that the two shapes are almost identical and that the entire history leading to this is thus the same and independent of the width parameter.

The general method described above was also applied to the case of an isothermal binary alloy. In order to obtain a hard check on the accuracy and performance of

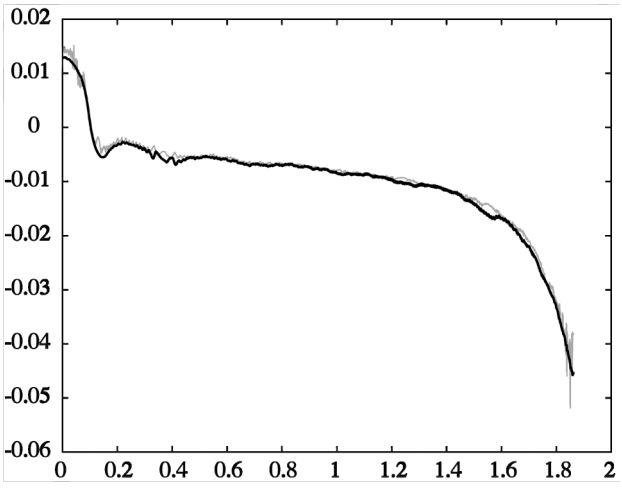

FIG. 2. The temperature on the interface from simulation (thick line) and the local Gibbs-Thomson relation (thin line).

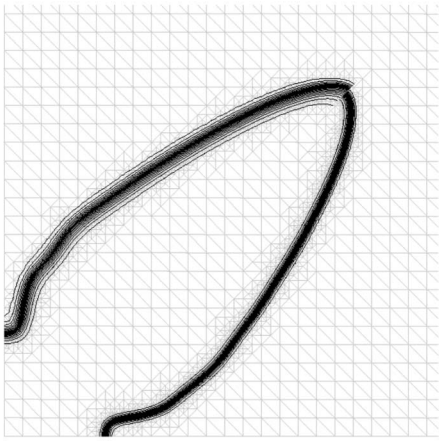

FIG. 3. Contours of the phase field variable obtained for $W = 0.04$ (above the diagonal), and $W = 0.02$ (below).

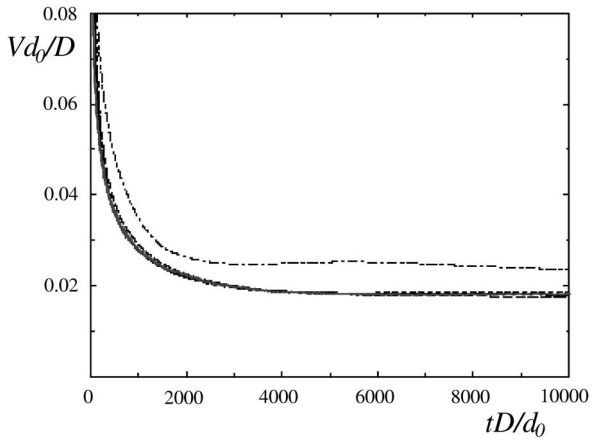

FIG. 4. The solid line shows present results ($\lambda = 8.396$), entirely coinciding with the antitrapping thin interface model [8] ($\lambda = 1.858$). Long dashed line: standard model from [8], ($\lambda = 1.858$). Short dashed line: antitrapping thin interface from [8], ($\lambda = 3.61$). Dash-dotted line: standard from [8], ($\lambda = 3.61$).

the method in this situation, we repeated a calculation reported in . The model consists of Eqs. (2) and (22) of [8], and this was implemented by replacing the temperature θ in Eq. (1), by $(e^u - 1)/(1 - k)$, where $u = \ln(\{2c/c_l^0\}/\{1 + k - (1 - k)[2g_\delta(\phi) - 1]\})$ is the chemical potential, k is the partition ratio, c is the concentration, and c_l^0 is the equilibrium liquid concentration. Equation (2) was replaced by the continuity equation for solute [Eq. (2) in [8]], with a diffusive flux $j = D_\delta(\phi)\nabla u$. The diffusion coefficient $D_\delta(\phi)$ tends to a step function as δ tends to zero.

$D_\delta(\phi)$ is chosen so that the step is displaced a distance proportional to δ into the solid. In the computations (made with $\delta = 0.05$) this means that the diffusion coefficient is constant in the region of size about one or two elements where $g_\delta(\phi)$ varies, and that the change in diffusion coefficient takes place 2–3 elements inside the solid. Another technicality is that the calculations reported in [8] were done at zero kinetic undercooling ($1/\mu = 0$). Here this was enforced by solving the equations implicitly, which also allowed a quite large time step.

Fig. 4 shows a direct comparison between our calculation and those presented in Fig. 1 in [8], showing the tip speed as a function of time for a case with scaled supersaturation $\Omega = 0.55$, $\epsilon = 0.02$, $k = 0.15$. In our simulation $\lambda = W/d_0 = 8.396$, the minimum mesh spacing was $h/d_0 = 0.42$, and the time step increased from $dtD/d_0 = 0.705$ initially, to 70.5 at the end of the simulation. As seen from Fig. 4 our tip speed agrees exactly over the entire history with that obtained in [8] for the thin interface limit with $\lambda = 1.858$.

Another important check was made in Fig. 2 in [8], where the concentration along the centerline of the dendrite is plotted. It is shown there that an inaccurate treatment of the varying diffusivity causes a large increase in the solid concentration. Also here our results match the antitrapping thin interface model.

In summary, we have presented a few simple modifications of the standard phase field model that allow the correct kinetics to be simulated with quite thick interfaces. The only restrictions are in terms of numerical resolution, and that radii of curvature should be larger than interface widths.

[1] R. Kobayashi, Bull. Jpn. Soc. Ind. Appl. Math. **1**, 22 (1991).
[2] O. Penrose and P. Fife, Physica (Amsterdam) **43D**, 44 (1990).
[3] S. H. Davis, *Theory of Solidification* (Cambridge University Press, Cambridge, U.K., 2001).
[4] G. Caginalp and W. Xie, Phys. Rev. E **48**, 1897 (1993).
[5] G. Caginalp and J. Jones, Ann. Phys. (N.Y.) **237**, 66 (1995).
[6] A. Karma and W.-J. Rappel, Phys. Rev. Lett. **77**, 4050 (1996).
[7] A. Karma and W.-J. Rappel, Phys. Rev. E **53**, R3017 (1996).
[8] A. Karma, Phys. Rev. Lett. **87**, 115701 (2001).
[9] J. Ramirez and C. Beckermann, in *Proceedings of the 41st AIAA Aerospace Sciences Meeting, Reno, NV, 2003* (American Institute of Aeronautics and Astronautics, Reston, VA, 2003).
[10] J. Bragard, A. Karma, Y. Lee, and M. Plapp, Interface Sci. **10**, 121 (2002).
[11] Y.-T. Kim, N. Goldenfeld, and J. Dantzig, Phys. Rev. E **62**, 2471 (2000).
[12] G. Amberg, R. Tönhardt, and C. Winkler, Math. Comput. Simul. **49**, 149 (1999).
[13] I. Loginova, G. Amberg, and J. Ågren, Acta Mater. **49**, 573 (2001).
[14] R. Tönhardt and G. Amberg, Phys. Rev. E **62**, 828 (2000).